Time domain analysis of non-Markovian Stochastic Petri Nets with PRI transitions *

András Horváth[1], Miklós Telek[2]
[1]Dipartimento di Informatica, Università di Torino
Corso Svizzera 185, 10149 Torino, Italy, *horvath@di.unito.it*
[2]Department of Telecommunications, Technical University of Budapest
Sztoczek u. 2, 1521 Budapest, Hungary, *telek@hit.bme.hu*

Abstract

The time domain analysis of non-Markovian Stochastic Petri Nets (NMSPNs) with preemptive repeat identical (pri) type transitions is considered in this paper. The set of "time domain" equations describing the evolution of the marking process is provided. The relation of the time domain and the formerly available transform domain description is discussed. Based on the time domain description of the process a simple numerical procedure is provided to analyze the transient behavior. Two examples are calculated to illustrate the proposed numerical method.

Keywords: Non-Markovian Stochastic Petri Nets, preemption policies, preemptive repeat identical (pri) type transition, time domain analysis.

1 Introduction

The transient behavior of NMSPNs was intensively studied through the last decade. A very important result of this line of research was the definition of possible preemption policies. The preemption policies of the transitions of a stochastic Petri net determine the stochastic behavior of the model.

The first works on stochastic Petri nets with non-exponentially distributed firing time already indicated that the stochastic behavior of these models are quite complex. The role of the preemption policy on this complex stochastic behavior was first studied in [1]. Three preemption policies were defined in [1]: *resampling*, *enabling* and *age*. These three policies allow exact analysis of the marking process when the firing time of the timed transitions are exponentially or continuous time Phase type distributed. The *resampling* policy implies a strict artificial restriction on the model behavior, hence this policy is quite rarely used in practical applications. The stochastic behavior of NMSPNs with *enabling*

*M. Telek gratefully acknowledges the support of OTKA T34972. A. Horváth gratefully acknowledges the support of the Italian Ministry for University and Scientific Research, through the Planet-IP project

and *age* preemption policy got higher attention. First the stochastic behavior of NMSPNs with *enabling* preemption policy and non-exponential firing time was obtained [2, 8, 12]. Some time later NMSPNs with *age* preemption policy was analyzed as well [6, 17, 18]. The applied analytical techniques (Markov renewal theory, supplementary variable approach) and the obtained results made it possible to define preemption policies in a more general framework. As a result a new preemption policy and a new terminology of the previously studied policies were introduced in [3]. Borrowing the terminology from queuing theory [16] the *enabling* preemption policy was referred to as preemptive repeat different (prd), the *age* policy as preemptive resume (prs) and the new one as preemptive repeat identical (pri).

The analytical description of the transient and steady state behavior of NMSPNs with pri transitions was considered in [3, 5, 4]. The common feature of these works is that the analysis is based on Markov renewal theory and the transient solution is provided in Laplace transform domain. Based on the transform domain description of the system behavior it was possible to obtain effective numerical analysis methods to calculate the steady state behavior [5]. On the other hand, since to get the transient probabilities numerical integration and inverse Laplace transformation had to be performed [3, 4], no effective transient analysis technique was found.

An alternative "time domain" approach for the transient analysis of NMSPNs with pri transitions was proposed in [15]. This approximate numerical method is based on the analysis of a DTMC over an expanded state space that is obtained by discretizing the time and the firing time distribution of the pri type transitions in the original (continuous time) model.

This paper provides the "time domain" analytical description of NMSPNs with pri transitions that was not available before. To obtain this result we apply a modified version of the supplementary variable approach [9]. The importance of this time domain analytical description is two-fold. First, it can verify the available approximate time domain analysis method. Second, it allows the development of sophisticated numerical methods of higher precision. The paper also shows the relation of the time domain process description with the formerly available Laplace transform domain one.

The rest of the paper is organized as follows. Section 2 provides the basic modeling assumptions and the applied notation. The main result of the paper, the analytical description of NMSPNs with pri type transitions is presented in Section 3. The relation of the time domain and the previously known transform domain description is discussed in Section 4. Based on the time domain description a first order numerical solution procedure is presented in Section 5. The numerical properties of the proposed method is studied through two examples in Section 6. The paper is concluded in Section 7.

2 Notation and modeling assumptions

For a detailed discussion on the definition of NMSPNs and the stochastic behavior of the different preemption policies we refer to [4]. Here we only summarize the behavior of pri type transitions and specify the subclass of NMSPNs which is considered in this paper.

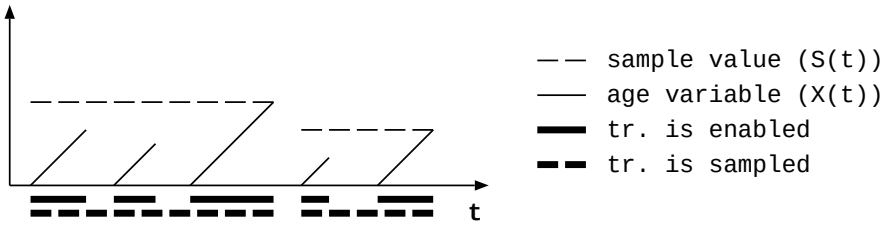

Figure 1: Sample value and age variable of a pri type transition

There are several possible interpretations of the behavior of a timed transition of a Petri net. The set of roles that defines the behavior of a transition in case of preemption is referred to as preemption policy. Preemption is the event when an enabled transition gets disabled before firing due to the firing of an other transition. The most natural interpretation with respect to the subsequent analytical discussion is the following. When a pri type transition gets enabled the first time after it has fired (or the very first time it gets enabled) a firing time sample is drawn from the firing time distribution of the transition. The transition fires when it is enabled continuously for a period of this firing time sample. Hence, at a given time instant the state of the transition is characterized by the firing time sample and the time for which the transition is continuously enabled (if the transition is disabled this value is 0). The former parameter is referred to as *sample value* and the latter one as *age variable*. From the instant of time when the firing sample is drawn to the firing of the transition we say that the pri type transition is *sampled*. Figure 1 gives a possible trajectory of the *sample value* and the *age variable* of a pri type transition and indicates those periods of time in which the transition is enabled or *sampled*.

As a consequence of the above explained behavior of pri type transitions, at a given time instant, if there is at least one sampled pri type transition the future evolution of the stochastic marking process depends on one or more continuous variables.

In this paper we consider a class of NMSPNs with the following properties. There are three kinds of transitions:

- prd and prs type transitions with exponentially distributed firing time are referred to as EXP transitions;
- transitions with pri policy and any general continuous firing time distribution (including exponentially distributed) are referred to as pri type transitions,
- and immediate transitions.

Note that the prd and the prs preemption policies are equivalent for transitions with exponentially distributed firing time [3]. G denotes the set of pri type transition. $\mathcal{S}$ is the set of tangible markings and $X(t) \in \mathcal{S}$ denotes the marking at time t; the marking process is assumed to be the right continuous. We assume that the sampling periods of the pri type transitions are distinct. The applied time domain analysis technique theoretically allows the analytical description of the system behavior also with overlapping sampled

periods at the expense of using more continuous variables in the state descriptors of the model. Furthermore, in the case of overlapping samples periods, additional attention is needed to handle the transitions between markings with 0, 1, 2,... sampled pri type transitions. For the above reasons, and because of the introduced numerical problems, the case of overlapping sampled periods is not considered in this paper.

The set of tangible markings $\mathcal{S}$ is partitioned into disjoint sets as follows:

$$\mathcal{S} = \mathcal{S}^M \cup \mathcal{S}^E \cup \mathcal{S}^D, \quad \mathcal{S}^E = \cup_{g \in G}\ \mathcal{S}^{\mathcal{E}_g} \text{ and } \mathcal{S}^D = \cup_{g \in G}\ \mathcal{S}^{\mathcal{D}_g},$$

where $\mathcal{S}^M$ is the set of marking in which non of the pri type transitions is sampled. $\mathcal{S}^E$ and $\mathcal{S}^D$ are the sets where the sampled pri type transition is enabled and disabled, respectively. $\mathcal{S}^E$ and $\mathcal{S}^D$ are further partitioned based on the particular sampled pri transition. Matrix $\boldsymbol{Q}$ of size $\mathcal{S} \times \mathcal{S}$ describes the state transition rates due to the firing of EXP transitions (this matrix takes into account the effect of immediate transitions that get enabled by the firing of an EXP transition). Matrix $\boldsymbol{\Delta}$ of size $\mathcal{S} \times \mathcal{S}$ contains the probabilities of state transitions by the firing of pri type transitions (taking into account the effect of immediate transitions activated by the firing of pri transitions). Matrices filtered according to the above state space partitioning are presented in the Appendix.

The probability density function of the firing time distribution of the pri type transition g is denoted by $f_g(x)$. To keep the subsequent discussion simpler, no immediate re-enabling of pri type transitions is considered; however, it would be possible to describe immediate re-enabling by the presented approach, but would require the introduction of additional matrices and would complicate the expressions.

3 Time domain model description

In order to describe the stochastic behavior of the process the following quantities are introduced:

- For those markings in which a pri type transition is enabled, the common cumulative density of the *age variable* $X(t)$ and the *sample value* $S(t)$ is defined as

$$\pi_i(t,x,y) = \frac{\partial^2}{\partial x \partial y} Pr(N(t) = i, X(t) \le x, S(t) \le y), \quad i \in \mathcal{S}^E. \tag{1}$$

  We compose a vector of these densities as (for the sake of simplicity, instead of giving the precise index of the components, we use the symbol $\bullet$)

$$\boldsymbol{\pi}^E(t,x,y) = \Big[\underbrace{0,\ldots,0}_{\mathcal{S}^M}, \underbrace{\pi_\bullet(t,x,y),\ldots,\pi_\bullet(t,x,y)}_{\mathcal{S}^{\mathcal{E}_1}}, \underbrace{0,\ldots,0}_{\mathcal{S}^{\mathcal{D}_1}}, \ldots,$$
$$\underbrace{\pi_\bullet(t,x,y),\ldots,\pi_\bullet(t,x,y)}_{\mathcal{S}^{\mathcal{E}_n}}, \underbrace{0,\ldots,0}_{\mathcal{S}^{\mathcal{D}_n}}\Big].$$

- For those states in which a pri type transition is sampled but disabled, the cumulative density of the *sample value* $S(t)$ is defined as

$$\pi_i(t,y) = \frac{\partial}{\partial y} Pr(N(t) = i, S(t) \leq y), \quad i \in \mathcal{S}^D. \tag{2}$$

The vector composed of these quantities has the form

$$\boldsymbol{\pi}^D(t,y) = \Big[\underbrace{0,\ldots,0}_{\mathcal{S}^M}, \underbrace{0,\ldots,0}_{\mathcal{S}^{\mathcal{E}_1}}, \underbrace{\pi_\bullet(t,y),\ldots,\pi_\bullet(t,y)}_{\mathcal{S}^{\mathcal{D}_1}}, \ldots, \underbrace{0,\ldots,0}_{\mathcal{S}^{\mathcal{E}_n}}, \underbrace{\pi_\bullet(t,y),\ldots,\pi_\bullet(t,y)}_{\mathcal{S}^{\mathcal{D}_n}} \Big] .$$

- Finally, the transient probabilities of those markings in which there is not sampled pri type transition are denoted by

$$\pi_i(t) = Pr(N(t) = i), \quad i \in \mathcal{S}^M. \tag{3}$$

The vector containing these probabilities is defined as

$$\boldsymbol{\pi}^M(t) = \Big[\underbrace{\pi_1(t),\ldots,\pi_\bullet(t)}_{\mathcal{S}^M}, \underbrace{0,\ldots,0}_{\mathcal{S}^{\mathcal{E}_1}}, \underbrace{0,\ldots,0}_{\mathcal{S}^{\mathcal{D}_1}}, \ldots, \underbrace{0,\ldots,0}_{\mathcal{S}^{\mathcal{E}_n}}, \underbrace{0,\ldots,0}_{\mathcal{S}^{\mathcal{D}_n}} \Big] .$$

As one could observe the above defined quantities are connected to the three different subsets of the markings $\mathcal{S}^E, \mathcal{S}^D$ and $\mathcal{S}^M$. The following three theorems describe the evolution of the process in the three subsets based on a modified version of the supplementary variable approach [9].

Theorem 1 *The evolution of the common cumulative density of the* age variable *and the* sample value *is described by the following partial differential equation for* $i \in \mathcal{S}^{\mathcal{E}_g}, g \in G, 0 < x < y$

$$\frac{\partial}{\partial t}\pi_i(t,x,y) + \frac{\partial}{\partial x}\pi_i(t,x,y) = \sum_{j \in \mathcal{S}^{\mathcal{E}_g}} \pi_j(t,x,y)\ q_{ji}. \tag{4}$$

Proof: For an infinitesimal period of time, during a sojourn in marking $i \in \mathcal{S}^{\mathcal{E}_g}$ while $0 < x < y$, the *age variable* $(X(t))$ grows at rate 1, the *sample value* $(S(t))$ remains unchanged and the sampled pri type transition may not fire. State transitions are possible only by a firing of an EXP transition. Hence

$$\begin{aligned} \pi_i(t+\delta,x,y) = \ & (1 + q_{ii}\delta)\pi_i(t,x-\delta,y) + \\ & \sum_{j \in \mathcal{S}^{\mathcal{E}_g}, j \neq i} \pi_j(t,x-\delta,y)\ q_{ji}\delta + \sigma(\delta)\ , \end{aligned} \tag{5}$$

where $\sigma(\delta)$ is such that $\lim_{\delta\to 0}\sigma(\delta)/\delta = 0$. Equation (4) is obtained from (5) by making the $\delta \to 0$ limit. □

Using matrix notation (4) may be written as

$$\frac{\partial}{\partial t}\boldsymbol{\pi}^E(t,x,y) + \frac{\partial}{\partial x}\boldsymbol{\pi}^E(t,x,y) = \boldsymbol{\pi}^E(t,x,y)\boldsymbol{Q}^E. \tag{6}$$

Theorem 2 *The evolution of the cumulative density of the* sample value $S(t)$ *for* $i \in \mathcal{S}^{\mathcal{D}_g}, g \in G$ *is described by the differential equation*

$$\begin{aligned}\frac{\partial}{\partial t}\pi_i(t,y) = \quad & \sum_{j\in\mathcal{S}^{\mathcal{D}_g}} \pi_j(t,y)\ q_{ji} + f^g(y)\sum_{j\in\mathcal{S}^M}\pi_j(t)\ q_{ji} + \\ & \sum_{j\in\mathcal{S}^{\mathcal{E}_g}}\int_{x=0}^{y}\pi_j(t,x,y)\ q_{ji}\ dx + f^g(y)\sum_{\ell\in G}\sum_{j\in\mathcal{S}^{\mathcal{E}_\ell}}\int_{x=0}^{\infty}\pi_j(t,x,x)\ dx\ \Delta_{ji}.\end{aligned} \tag{7}$$

Proof: Marking $i \in \mathcal{S}^{\mathcal{D}_g}$ with *sample value* y is reachable at time $t+\delta$ in the following ways:

- there is no state transition between t and $t+\delta$ and the *sample value* is y at time t,
- there is a state transitions inside $\mathcal{S}^{\mathcal{D}_g}$ between t and $t+\delta$ by the firing of an EXP transition and the *sample value* is y at time t,
- there is a state transition from $\mathcal{S}^M$ to i between t and $t+\delta$ and the new *sample value* of t_g is y,
- there is a state transitions from $\mathcal{S}^{\mathcal{E}_g}$ to i due to the firing of an EXP transition between t and $t+\delta$ and the *sample value* is y at time t (i.e., the enabled pri type transition whose *sample value* is y gets disabled),
- one of the pri type transitions fires between t and $t+\delta$ (i.e., the value of its age variable reaches the value of the firing time sample), the new state after the firing is i and the new *sample value* of the considered transition is y,
- or more than one state transitions occur between t and $t+\delta$.

Considering these cases we have

$$\begin{aligned}\pi_i(t+\delta,y) = \quad & (1+q_{ii}\delta)\pi_i(t,y) + \\ & \sum_{j\in\mathcal{S}^{\mathcal{D}_g}, j\neq i}\pi_j(t,y)\ q_{ji}\delta + f^g(y)\sum_{j\in\mathcal{S}^M}\pi_j(t)\ q_{ji}\delta + \\ & \sum_{j\in\mathcal{S}^{\mathcal{E}_g}}\frac{\partial}{\partial y}Pr(N(t)=j, X(t)<S(t)-\delta, S(t)\le y)q_{ji}\delta + \\ & f^g(y)\sum_{\ell\in G}\sum_{j\in\mathcal{S}^{\mathcal{E}_\ell}}Pr(N(t)=j, S(t)-\delta<X(t))\ \Delta_{ji}\ + \sigma(\delta).\end{aligned} \tag{8}$$

Theorem 2 is obtained as $\delta \to 0$. □

Based on (7) we also have the firing frequency (or firing rate) at which the pri type transition t_g fires in state $i \in \mathcal{S}^{\mathcal{E}_g}$ at time t:

$$\begin{aligned} \varphi_i(t) &= \lim_{\delta \to 0} \frac{Pr(t_g \text{ fires in state } i \text{ during } (t, t+\delta))}{\delta} \\ &= \lim_{\delta \to 0} \frac{Pr(X(t) = i, S(t) - \delta < X(t)) + \sigma(\delta)}{\delta} \\ &= \int_{y=0}^{\infty} \pi_i(t, y, y)\ dy. \end{aligned} \tag{9}$$

The vector composed by these elements is

$$\boldsymbol{\varphi}(t) = \left[\underbrace{0, \ldots, 0}_{\mathcal{S}^M}, \underbrace{\varphi_\bullet(t), \ldots, \varphi_\bullet(t)}_{\mathcal{S}^{\mathcal{E}_1}}, \underbrace{0, \ldots, 0}_{\mathcal{S}^{\mathcal{D}_1}}, \ldots, \underbrace{\varphi_\bullet(t), \ldots, \varphi_\bullet(t)}_{\mathcal{S}^{\mathcal{E}_n}}, \underbrace{0, \ldots, 0}_{\mathcal{S}^{\mathcal{D}_n}} \right].$$

Using matrix notation (7) becomes

$$\begin{aligned} \frac{\partial}{\partial t} \boldsymbol{\pi}^D(t, y) = \ & \boldsymbol{\pi}^M(t) \boldsymbol{Q}^{MD} \boldsymbol{f}(y) + \boldsymbol{\pi}^D(t, y) \boldsymbol{Q}^D + \\ & \boldsymbol{\varphi}(t) \boldsymbol{\Delta}^D \boldsymbol{f}(y) + \int_{x=0}^{y} \boldsymbol{\pi}^E(t, x, y)\ dx\ \boldsymbol{Q}^{ED}. \end{aligned} \tag{10}$$

Theorem 3 *The transient probabilities of the markings in $\mathcal{S}^M$, $i \in \mathcal{S}^M$, satisfies the differential equation*

$$\frac{\partial}{\partial t} \pi_i(t) = \sum_{j \in \mathcal{S}^M} \pi_j(t)\ q_{ji} + \sum_{\ell \in G} \sum_{j \in \mathcal{S}^{\mathcal{E}_\ell}} \int_{x=0}^{\infty} \pi_j(t, x, x) dx \Delta_{ji}. \tag{11}$$

Proof: Marking $i \in \mathcal{S}^M$ is reachable at time $t + \delta$ in the following ways:

- there is no state transition between t and $t + \delta$,
- there is a state transitions inside $\mathcal{S}^M$ between t and $t + \delta$ by the firing of an EXP transition,
- one of the pri type transitions fires between t and $t + \delta$ and the new state after the firing is i,
- more than one state transitions occur between t and $t + \delta$.

These possible cases results

$$\begin{aligned} \pi_i(t + \delta) = \ & (1 + q_{ii}\delta)\pi_i(t) + \sum_{j \in \mathcal{S}^M, j \neq i} \pi_j(t)\ q_{ji}\delta + \\ & f^g(y) \sum_{\ell \in G} \sum_{j \in \mathcal{S}^{\mathcal{E}_\ell}} Pr(N(t) = j, S(t) - \delta < X(t))\ \Delta_{ji} + \sigma(\delta). \end{aligned} \tag{12}$$

Theorem 3 is obtained as $\delta \to 0$. □

Using matrix notation (11) may be written as

$$\frac{\partial}{\partial t}\boldsymbol{\pi}^M(t) = \boldsymbol{\pi}^M(t)\boldsymbol{Q}^M + \boldsymbol{\varphi}(t)\boldsymbol{\Delta}^M. \tag{13}$$

In order to have a complete description of the system one has to define the boundary conditions. It is given in the following theorem.

Theorem 4 *The initial value of* $\pi_i(t,0,y)$, $i \in \mathcal{S}^{\mathcal{E}_g}, g \in G$ *is described by the equation*

$$\begin{aligned}\pi_i(t,0,y) = & \sum_{j\in\mathcal{S}^{\mathcal{D}_g}} \pi_j(t,y)\ q_{ji} + f^g(y) \sum_{j\in\mathcal{S}^M} \pi_j(t)\ q_{ji} + \\ & f^g(y) \sum_{\ell\in G}\sum_{j\in\mathcal{S}^{\mathcal{E}_\ell}} \int_{x=0}^{\infty} \pi_j(t,x,x)\ dx\ \Delta_{ji}.\end{aligned} \tag{14}$$

Proof: By the definition of $\pi_i(t,x,y)$

$$\pi_i(t,0,y) = \lim_{\delta\to 0} \frac{\dfrac{\partial}{\partial y} Pr(N(t+\delta)=i, X(t+\delta)<\delta, S(t+\delta)\le y)}{\delta}\ , \tag{15}$$

hence we consider the possible cases that results in marking $i \in \mathcal{S}^{\mathcal{E}_g}, g \in G$ at time $t+\delta$ with *sample value* y and *age variable* less than δ:

- there is a state transitions from $\mathcal{S}^{\mathcal{D}_g}$ to i between t and $t+\delta$ by the firing of an EXP transition and the *sample value* is y at time t,
- there is a state transition from $\mathcal{S}^M$ to i between t and $t+\delta$ and the new *sample value* of t_g is y,
- one of the pri type transitions fires between t and $t+\delta$ the new state after the firing is i and the new *sample value* of t_g is y,
- or more than one state transitions occur between t and $t+\delta$.

Considering these cases we have

$$\begin{aligned}&\frac{\partial}{\partial y} Pr(N(t+\delta)=i,\ X(t+\delta)<\delta, S(t+\delta)\le y) = \\ &\qquad \sum_{j\in\mathcal{S}^{\mathcal{D}_g}} \pi_j(t,y)\ q_{ji}\delta + f^g(y) \sum_{j\in\mathcal{S}^M} \pi_j(t)\ q_{ji}\delta + \\ &\qquad f^g(y) \sum_{\ell\in G}\sum_{j\in\mathcal{S}^{\mathcal{E}_\ell}} Pr(N(t)=j, S(t)-\delta<X(t))\ \Delta_{ji} + \sigma(\delta)\end{aligned} \tag{16}$$

Theorem 4 is obtained based on (15) and (16). □

Using matrix notation the boundary conditions (14) may be written as

$$\boldsymbol{\pi}^E(t,0,y) = \boldsymbol{\pi}^D(t,y)\boldsymbol{Q}^{DE} + \boldsymbol{\pi}^M(t)\boldsymbol{Q}^{ME}\boldsymbol{f}(y) + \boldsymbol{\varphi}(t)\boldsymbol{\Delta}^E\boldsymbol{f}(y). \tag{17}$$

The following section discusses the relation of the above introduced time domain description with the formerly known Laplace transform domain one. A numerical method based on this time domain equations is proposed in Section 5.

4 Relation of the MRGP and the time domain description

Unfortunately, the solution of (4)-(17) can not be obtained in transform domain as it was possible for NMSPNs with prd and prs transitions in [13]. Hence the relation of the time domain and the transform domain solution can not be obtained for the whole marking process. Instead, in order to show the relation of the Markov regenerative process (MRGP) approach and the time domain description provided by (4)-(17), we describe the evolution of the marking process during a regenerative period in which a pri type transition is sampled. The identity of the two approaches for Markovian regenerative periods in which only EXP transitions are enabled is not discussed here. It is an obvious consequence of [13].

In the following analysis, we reconsider those terms of (4)-(17) that describe the evolution of the subordinated process during a regenerative period associated with the pri type transition $g \in G$. (The subordinated process of the MRGP is equivalent to the sampled period of the pri type transition.) Then we show that the entries of the global and the local kernel of the MRGP associated with this regenerative period are identical to the ones obtained from the Markov regenerative approach in [3, 4]. To this end we assume that the marking process starts from state $i \in \mathcal{S}^{\mathcal{E}_g}$ at time 0. Since we are interested only in the subordinated process starting from $i \in \mathcal{S}^{\mathcal{E}_g}$ we consider the process evolution only in $\mathcal{S}^{\mathcal{E}_g} \cup \mathcal{S}^{\mathcal{D}_g}$ (note that during the regenerative period the process can not leave $\mathcal{S}^{\mathcal{E}_g} \cup \mathcal{S}^{\mathcal{D}_g}$.)

In the rest of the section, in order to simplify the notation, we avoid subscript g, the reference to the particular pri type transition.

Equations describing the process evaluation until the next firing of a *pri* transition are

$$\frac{\partial}{\partial t}\boldsymbol{\pi}^{\mathcal{E}}(t,x,y) + \frac{\partial}{\partial x}\boldsymbol{\pi}^{\mathcal{E}}(t,x,y) = \boldsymbol{\pi}^{\mathcal{E}}(t,x,y)\mathbf{Q}^{\mathcal{E}}, \tag{18}$$

$$\frac{\partial}{\partial t}\boldsymbol{\pi}^{\mathcal{D}}(t,y) = \boldsymbol{\pi}^{\mathcal{D}}(t,y)\boldsymbol{Q}^{\mathcal{D}} + \int_{x=0}^{y} \boldsymbol{\pi}^{\mathcal{E}}(t,x,y)\, dx\, \boldsymbol{Q}^{\mathcal{E}\mathcal{D}}, \tag{19}$$

$$\boldsymbol{\pi}^{\mathcal{E}}(t,0,y) = \boldsymbol{\pi}^{\mathcal{D}}(t,y)\boldsymbol{Q}^{\mathcal{D}\mathcal{E}}. \tag{20}$$

For $i \in \mathcal{S}^{\mathcal{E}}$ the firing frequency is defined as before:

$$\boldsymbol{\varphi}^{\mathcal{E}}(t) = \int_{y=0}^{\infty} \boldsymbol{\pi}^{\mathcal{E}}(t,y,y)\, dy. \tag{21}$$

Entries of the local and the global kernel of a MRGP are defined as

$$e_{ij}(t) = Pr(N(t) = j, T_1 > t \mid N(0) = i), \tag{22}$$

$$k_{ij}(t) = Pr(N(T_1^+) = j, T_1 \leq t \mid N(0) = i). \tag{23}$$

Setting the initial probability vector $\boldsymbol{\pi}_0^{\mathcal{E}} = [0, \ldots, 1, \ldots, 0]$ the vectors of the above kernel elements ($\boldsymbol{e}_i^{\mathcal{E}}(t) = \{e_{ij}(t)\}|_{j\in\mathcal{E}}$, $\boldsymbol{e}_i^{\mathcal{D}}(t) = \{e_{ij}(t)\}|_{j\in\mathcal{D}}$, and $\boldsymbol{k}_i^{\mathcal{E}}(t) = \{k_{ij}(t)\}|_{j\in S}$) are given by

$$\boldsymbol{e}_i^{\mathcal{E}}(t) = \int_{y=0}^{\infty}\int_{x=0}^{y} \boldsymbol{\pi}^{\mathcal{E}}(t,x,y)\; dxdy, \tag{24}$$

$$\boldsymbol{e}_i^{\mathcal{D}}(t) = \int_{y=0}^{\infty} \boldsymbol{\pi}^{\mathcal{D}}(t,y)\; dy, \tag{25}$$

$$\boldsymbol{k}_i(t) = \int_{0}^{t} \boldsymbol{\varphi}^{\mathcal{E}}(t)dt\boldsymbol{\Delta}, \tag{26}$$

where $\boldsymbol{\pi}^{\mathcal{E}}(t,x,y)$, $\boldsymbol{\pi}^{\mathcal{D}}(t,y)$ and $\boldsymbol{\varphi}^{\mathcal{E}}(t)$ are defined by (18)-(21).

The relation with the Markov regenerative approach is obtained in Laplace-transform domain. Transforming (18) twice, using $\boldsymbol{\pi}^{\mathcal{E}}(0,x,y) = \delta(x)\; f(y)\; \boldsymbol{\pi}_0^{\mathcal{E}}$, rearranging and inverse transforming with respect to x leads to

$$\boldsymbol{\pi}^{\mathcal{E}*}(s,x,y) = \left[\boldsymbol{\pi}_0^{\mathcal{E}}\; f(y) + \boldsymbol{\pi}^{\mathcal{E}*}(s,0,y)\right]\; e^{-\left(s\boldsymbol{I}^{\mathcal{E}} - \boldsymbol{Q}^{\mathcal{E}}\right)x}. \tag{27}$$

Transforming (19) using $\boldsymbol{\pi}^{\mathcal{D}}(0,y) = 0$ results

$$\boldsymbol{\pi}^{\mathcal{D}*}(s,y)\left(s\boldsymbol{I}^{\mathcal{D}} - \boldsymbol{Q}^{\mathcal{D}}\right) = \int_{x=0}^{y} \boldsymbol{\pi}^{\mathcal{E}*}(s,x,y)\; dx\; \boldsymbol{Q}^{\mathcal{E}\mathcal{D}}, \tag{28}$$

and from (20)

$$\boldsymbol{\pi}^{\mathcal{E}*}(s,0,y) = \boldsymbol{\pi}^{\mathcal{D}*}(s,y)\boldsymbol{Q}^{\mathcal{D}\mathcal{E}}. \tag{29}$$

Integrating (27) and inserting it to (28) results

$$\boldsymbol{\pi}^{\mathcal{D}*}(s,y)\left(s\boldsymbol{I}^{\mathcal{D}} - \boldsymbol{Q}^{\mathcal{D}}\right) = \left[\boldsymbol{\pi}_0^{\mathcal{E}}\; f(y) + \boldsymbol{\pi}^{\mathcal{E}*}(s,0,y)\right]\int_{x=0}^{y} e^{-\left(s\boldsymbol{I}^{\mathcal{E}} - \boldsymbol{Q}^{\mathcal{E}}\right)x}\; dx\; \boldsymbol{Q}^{\mathcal{E}\mathcal{D}}, \tag{30}$$

Using the notation

$$\boldsymbol{P}^{\mathcal{E}\mathcal{D}}(s,y) = \int_{x=0}^{y} e^{-\left(s\boldsymbol{I}^{\mathcal{E}} - \boldsymbol{Q}^{\mathcal{E}}\right)x} dx\; \boldsymbol{Q}^{\mathcal{E}\mathcal{D}}$$

we have

$$\boldsymbol{\pi}^{\mathcal{D}*}(s,y) = \left[\boldsymbol{\pi}_0^{\mathcal{E}}\; f(y) + \boldsymbol{\pi}^{\mathcal{E}*}(s,0,y)\right]\boldsymbol{P}^{\mathcal{E}\mathcal{D}}(s,y)\left(s\boldsymbol{I}^{\mathcal{D}} - \boldsymbol{Q}^{\mathcal{D}}\right)^{-1}. \tag{31}$$

Using the notation $\boldsymbol{P}^{\mathcal{D}\mathcal{E}}(s) = \left(s\boldsymbol{I}^{\mathcal{D}} - \boldsymbol{Q}^{\mathcal{D}}\right)^{-1}\boldsymbol{Q}^{\mathcal{D}\mathcal{E}}$, from (29) and (31) we have

$$\boldsymbol{\pi}^{\mathcal{E}*}(s,0,y) = \left[\boldsymbol{\pi}_0^{\mathcal{E}}\; f(y) + \boldsymbol{\pi}^{\mathcal{E}*}(s,0,y)\right]\boldsymbol{P}^{\mathcal{E}\mathcal{D}}(s,y)\boldsymbol{P}^{\mathcal{D}\mathcal{E}}(s). \tag{32}$$

Adding $\boldsymbol{\pi}_0^{\mathcal{E}}\ f(y)$ to both sides and rearranging the result we have

$$\boldsymbol{\pi}_0^{\mathcal{E}}\ f(y) + \boldsymbol{\pi}^{\mathcal{E}*}(s,0,y) = \boldsymbol{\pi}_0^{\mathcal{E}}\ f(y)\left[\boldsymbol{I}^{\mathcal{E}} - \boldsymbol{P}^{\mathcal{E}\mathcal{D}}(s,y)\boldsymbol{P}^{\mathcal{D}\mathcal{E}}(s)\right]^{-1}. \tag{33}$$

Finally, from (27) and (33)

$$\begin{aligned}\boldsymbol{e}_i^{\mathcal{E}*}(s) = &\int_{y=0}^{\infty}\int_{x=0}^{y}\boldsymbol{\pi}^{\mathcal{E}*}(s,x,y)\ dxdy = \\ &\boldsymbol{\pi}_0^{\mathcal{E}}\int_{y=0}^{\infty} f(y)\left[\boldsymbol{I}^{\mathcal{E}} - \boldsymbol{P}^{\mathcal{E}\mathcal{D}}(s,y)\boldsymbol{P}^{\mathcal{D}\mathcal{E}}(s)\right]^{-1}\cdot\int_{x=0}^{y} e^{-\left({}_s\boldsymbol{I}^{\mathcal{E}}-\boldsymbol{Q}^{\mathcal{E}}\right)x}\ dxdy,\end{aligned} \tag{34}$$

$$\begin{aligned}\boldsymbol{e}_i^{\mathcal{D}*}(s) = &\int_{y=0}^{\infty}\boldsymbol{\pi}^{\mathcal{D}*}(s,y)\ dy = \\ &\boldsymbol{\pi}_0^{\mathcal{E}}\int_{y=0}^{\infty} f(y)\left[\boldsymbol{I}^{\mathcal{E}} - \boldsymbol{P}^{\mathcal{E}\mathcal{D}}(s,y)\boldsymbol{P}^{\mathcal{D}\mathcal{E}}(s)\right]^{-1}\cdot\boldsymbol{P}^{\mathcal{E}\mathcal{D}}(s,y)\left(s\boldsymbol{I}^{\mathcal{D}} - \boldsymbol{Q}^{\mathcal{D}}\right)^{-1}\ dy,\end{aligned} \tag{35}$$

$$\begin{aligned}\boldsymbol{k}_i^{*}(s) = &\frac{1}{s}\ \boldsymbol{\varphi}^{\mathcal{E}*}(s)\boldsymbol{\Delta} = \\ &\frac{1}{s}\ \boldsymbol{\pi}_0^{\mathcal{E}}\int_{y=0}^{\infty} f(y)\left[\boldsymbol{I}^{\mathcal{E}} - \boldsymbol{P}^{\mathcal{E}\mathcal{D}}(s,y)\boldsymbol{P}^{\mathcal{D}\mathcal{E}}(s)\right]^{-1}\cdot e^{-\left({}_s\boldsymbol{I}^{\mathcal{E}}-\boldsymbol{Q}^{\mathcal{E}}\right)y}\ dy.\end{aligned} \tag{36}$$

Equations (34) - (36) show a perfect coincidence with the results presented in [4].

5 A numerical method based on time domain description

In this section, we introduce a simple numerical method to approximate the stochastic behavior described by the above set of equations. The proposed method is similar to algorithms used for the analysis of NMSPNs with prd [11] and prs [18] type transitions. We use an equidistant discretization of the time, the age and the sample value. The discretization step is denoted by d. The proposed method is a first order forward approximation of the process evolution described by Equations (4)-(17). The proposed method is applicable only if the pri type transition has a finite firing time distribution. The finite truncation of an infinite support firing time distribution can result in very poor approximation even in the case of distributions with exponentially decaying tail [7]. The mean time of a regenerative period associated with a pri type transition might become infinite [7] and this feature is lost by any kind of finite truncation of the firing time.

The initial values of the numerical procedure are set based on the initial marking of the net ($\boldsymbol{\pi}_0 = \{Pr(N(0) = i)\}$), and on the firing time distribution of the pri type transitions ($\boldsymbol{f}(y)$):

- for $\mathcal{S}^M$: $\boldsymbol{\pi}^M(0) = \boldsymbol{\pi}_0^M$,

- for $\mathcal{S}^E$: $\boldsymbol{\pi}^E(0,0,kd) = \boldsymbol{\pi}_0^E \boldsymbol{D}(k,d),\ k \geq 1$, and $\boldsymbol{\pi}^E(0,md,kd) = 0,\ m \geq 1, k \geq 1$,
- for $\mathcal{S}^D$: $\boldsymbol{\pi}^D(0,kd) = \boldsymbol{\pi}_0^D \boldsymbol{D}(k,d),\ k \geq 1$,

where $\boldsymbol{D}(k,d) = \int_{y=(k-1)d}^{kd} \boldsymbol{f}(y)dy$.

The transient behavior of the marking process at time nd is calculated by the following steps:

1. Compute $\boldsymbol{\pi}^E(nd,md,kd)$ for $n \geq 1$ and $k > m > 0$ based on the process evolution in $\mathcal{S}^E$ during $((n-1)d, nd)$ using (6):

$$\boldsymbol{\pi}^E(nd,md,kd) = \boldsymbol{\pi}^E((n-1)d,(m-1)d,kd)\ e^{\boldsymbol{Q}^E d}.$$

   The matrix $e^{\boldsymbol{Q}^E d}$ contains the state transition probabilities of the marking process for the $((n-1)d, nd)$ interval (considering an unlimited number of state transitions due to the firing of EXP transition) suppose the marking process stays in $\mathcal{S}^E$.

2. Compute the firing rate based on (9):

$$\boldsymbol{\varphi}(nd) = \sum_{k=1}^{k_{max}} \boldsymbol{\pi}^E((n-1)d,(k-1)d,kd)\ e^{\boldsymbol{Q}^E d},$$

   where k_{max} is calculated based on the largest considered firing time of the pri type transitions.

3. Compute $\boldsymbol{\pi}^D(nd,kd)$ for $n \geq 1$ based on (10):

$$\begin{aligned}\boldsymbol{\pi}^D(nd,kd) = \ & \boldsymbol{\pi}^D((n-1)d,kd)\ e^{\boldsymbol{Q}^D d} + \\ & \boldsymbol{\pi}^M((n-1)d)\ \boldsymbol{L}^M(d)\boldsymbol{Q}^{MD}\ \boldsymbol{D}(k,d) + \\ & \boldsymbol{\varphi}(nd)\boldsymbol{\Delta}^D\ \boldsymbol{D}(k,d) + \\ & \sum_{m=1}^{k-1} \boldsymbol{\pi}^E((n-1)d,md,kd)\ \boldsymbol{L}^E(d)\boldsymbol{Q}^{ED}\ \boldsymbol{D}(k,d)\ ,\end{aligned}$$

   where $\boldsymbol{L}^M(d) = \int_0^d e^{\boldsymbol{Q}^M t}\ dt$, and $\boldsymbol{L}^E(d)$ and $\boldsymbol{L}^D(d)$ are defined similarly.

4. Compute $\boldsymbol{\pi}^M(nd)$ for $n \geq 1$ based on (13):

$$\boldsymbol{\pi}^M(nd) = \boldsymbol{\pi}^M((n-1)d)\ e^{\boldsymbol{Q}^M d} + \boldsymbol{\varphi}(nd)\boldsymbol{\Delta}^M\ ,$$

5. Compute $\boldsymbol{\pi}^E(nd,0,kd)$ for $n \geq 1$ based on (17):

$$\begin{aligned}\boldsymbol{\pi}^E(nd,0,kd) = \ & \boldsymbol{\pi}^D((n-1)d,kd)\ \boldsymbol{L}^D(d)\boldsymbol{Q}^{DE} + \\ & \boldsymbol{\pi}^M((n-1)d)\ \boldsymbol{L}^M(d)\boldsymbol{Q}^{ME}\ \boldsymbol{D}(k,d) + \\ & \boldsymbol{\varphi}(nd)\boldsymbol{\Delta}^E\ \boldsymbol{D}(k,d)\ .\end{aligned}$$

The iterative application of these computational steps provides the transient behavior of a NMSPN. The state probabilities in $\mathcal{S}^E$ and $\mathcal{S}^D$ at time nd are calculated as follows:

$$\boldsymbol{\pi}^E(nd) = \sum_{k=1}^{k_{max}} \sum_{m=0}^{k-1} \boldsymbol{\pi}^E(nd, md, kd) \quad \text{and}$$

$$\boldsymbol{\pi}^D(nd) = \sum_{k=1}^{k_{max}} \boldsymbol{\pi}^D(nd, kd) \ .$$

5.1 Computational complexity and precision

The computing cost of an iteration step of this method is similar to a vector matrix multiplication. The numerical method can be viewed as the large vector, $\boldsymbol{\pi}(0)$ (containing all the vector elements associated with the $\mathcal{S}^M$, $\mathcal{S}^D$ and $\mathcal{S}^E$ subsets), is consecutively multiplied with a square matrix of the same cardinality. Depending mainly on the structure of the branching probability ($\boldsymbol{\Delta}$) and the generator matrix ($\boldsymbol{Q}$), the "multiplying matrix" is fairly sparse if the $\mathcal{S}^M$, $\mathcal{S}^{\mathcal{E}_g}$ and $\mathcal{S}^{\mathcal{D}_g}$ subsets are "small". E.g., during a sojourn in $\mathcal{S}^M$ the marking process evolves as a CTMC with generator $\boldsymbol{Q}^M$. If $\mathcal{S}^M$ forms a single irreducible set each state of $\mathcal{S}^M$ are reachable with positive probability in a d long interval, which means that the block of the "multiplying matrix" describes the state transitions in $\mathcal{S}^M$ contains only non-zero elements. To reduce the computational complexity we approximate $e^{\boldsymbol{Q}^M d}$ with $I + \boldsymbol{Q}^M d$ for large, connected $\mathcal{S}^M$ and sufficiently small d. The approximate $I + \boldsymbol{Q}^M d$ matrix is as sparse as $\boldsymbol{Q}^M$ is. The blocks of the "multiplying matrix" describing transitions from $\mathcal{S}^M$ to $\mathcal{S}^E$ or $\mathcal{S}^D$ and among the $\mathcal{S}^{\mathcal{E}_g}$, $\mathcal{S}^{\mathcal{D}_g}$ sets are usually sparse since only a limited number of transition firing enables a pri type transition in common models. The branching probability matrix ($\boldsymbol{\Delta}$) of an NMSPN with only timed transitions containes only one non-zero elements in each row. The presence of immediate transitions activated by the firing of pri type transitions might increase the number of non-zero elements in $\boldsymbol{\Delta}$.

The main difficulty of the introduced computational method is that the $\boldsymbol{\pi}(nd)$ vector easily becomes very large and hence, it has a high memory requirement to store two vectors of this size. The computational complexity, the number of floating point multiplication and summation in an iteration step, is computable from the cardinality of the $\boldsymbol{\pi}(nd)$ vector, $\#\boldsymbol{\pi}(nd)$, and the sparseness (# non-zero elements/# elements) of the "multiplying matrix", σ. It is $(\#\boldsymbol{\pi}(nd))^2\sigma$.

The main error of the applied numerical approach caused by the applied discrete representation of continuous quantities like the firing time distribution and the age distribution. There are different approaches proposed for this discretization assuming equidistant steps. An iterative method is proposed in [10] which represents the density value of continuous quantities at discrete points, and a direct method is proposed in [18] where discrete distributions are assumed at each time points. The introduced numerical method is of the second type because its computational complexity is less.

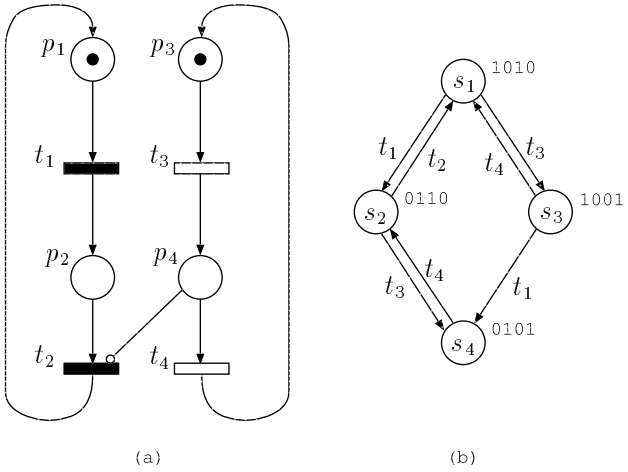

Figure 2: *PN* model of the terminal system

6 Numerical example

In this section, we demonstrate the applicability of the method and the role of preemption policies with numerical examples.

6.1 Terminal system

The first example is a model that served in several papers as an introductory example to present solution techniques for NMSPNs.

The *SPN* of Figure 2a models a system of 2 terminals. The jobs submitted by terminal 2 have higher priority and preempt the jobs submitted by terminal 1. The server adopts a *pri* service discipline, i.e., the work done before the preemption is lost and when the server becomes available again it has to perform a job of the same size as before. Place p_1 (p_3) signifies that terminal 1 (2) is in the thinking phase, while place p_2 (p_4) indicates job from terminal 1 (2) under service. Transition t_1 and t_3 model the submission of a job of type 1 or 2. Transition t_1 has deterministic firing time. Transition t_1 can not be preempted before firing, hence the preemptive policy of t_1 does not play any role. The firing time of t_3 is exponentially distributed. Transition t_2 is a pri type transition and represents the completion of service of the lower priority job (coming from terminal 1). The firing time of transition t_2 is assumed to be uniformly distributed with a *pri* preemptive policy. Transition t_4 models the service time of a higher priority job. Its firing time is exponentially distributed. The inhibitor arc from p_4 to t_2 models the described priority mechanism: as soon as a job from terminal 2 is submitted for processing, the job from terminal 1 under service (if any) is interrupted. After the higher priority is processed, the service of the same lower priority job is restarted from the beginning. The associated reachability graph is shown in Figure 2b.

The transient probabilities of this model were calculated assuming the following values:

- the firing time of the deterministic transition t_1 is 0.5;

- the firing rates of EXP transitions t_3 and t_4 are $\lambda_3 = 0.5$ and $\lambda_4 = 1$;
- the service time of a lower priority job (transition t_2) is uniformly distributed on the interval $[0.5, 1.5]$;
- the step size of discretization is $d = 0.002$.

Figure 3 and 4 depict the transient probabilities of the system states. The thicker curves are obtained by the procedure described in Section 5; the thiner ones are given by performing inverse Laplace transformation. As one can observe the inverse transform solution fails to follow the sharp changes of the transient probabilities; at times even negative probabilities are obtained. Instead, as verified by simulation the proposed discretization gives highly precise results.

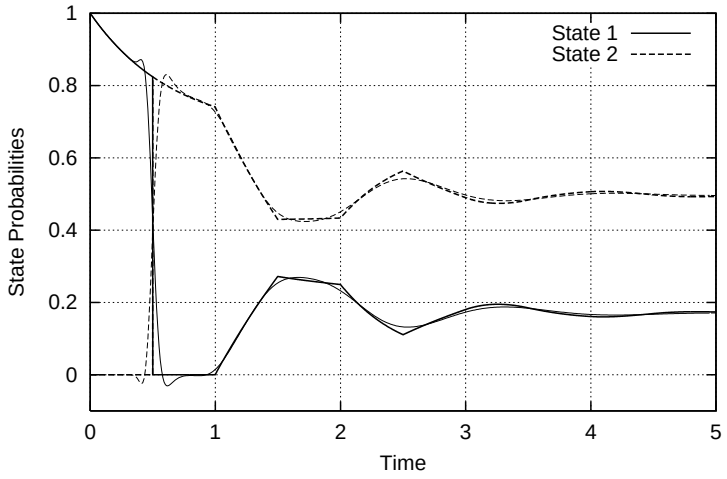

Figure 3: Transient state probabilities of the terminal system (state

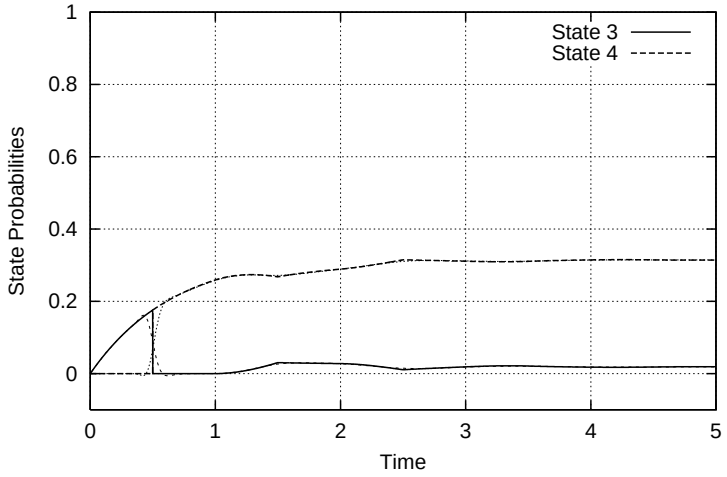

Figure 4: Transient state probabilities of the terminal system

The connection between the accuracy of the computations and the discretization step is illustrated in Figure 5 where the sum of the relative errors of the steady state probabilities against the discretization step is depicted (steady state results were calculated by performing transient analysis until the point where the probabilities assigned to the discretized state space do not change anymore).

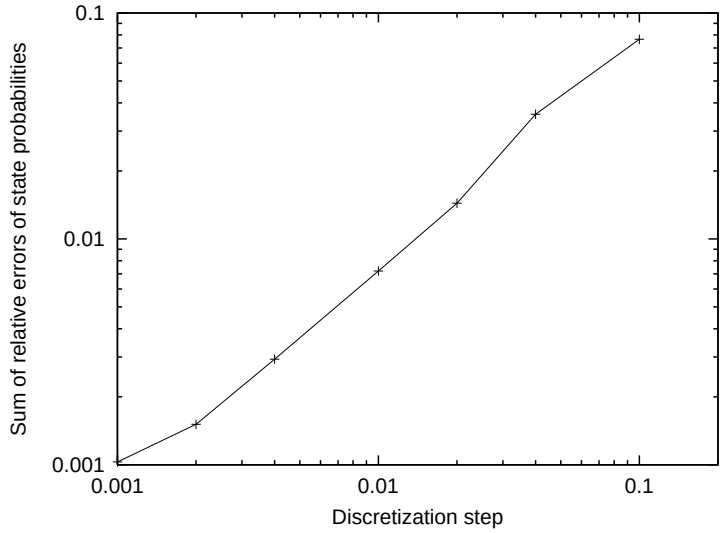

Figure 5: Sum of relative error of steady state probabilities

The size of the discretized state space is 251502. During the transient analysis, the vector matrix multiplication is performed 5/0.002=2500 times. The computations, executed on a computer running at 300 MHz with 256 Mbytes of main memory, took about 4 minutes.

6.2 The effect of preemption policy

To indicate the essential role of preemption policies in stochastic models we evaluate the stationary behaviour of the considered terminal system in the special case, when the thinking time of terminal 2 and the execution time of type 2 jobs are also exponentially distributed. Due to the memoryless property of the exponential distribution the prd and the prs preemption policy has the same effect [3]. In this example the prd and the prs preemption policy results in a 4-state CTMC marking process, since all firing times are exponentially distributed [7]. Instead, when pri preemption policy is assigned with transition t_2 the marking process is non-Markovian even all firing times are exponentially distributed [3]. It means that different preemption policies result significant qualitative difference in the underlying stochastic models [16]. The subsequent numerical analysis of the terminal system indicates that the preemption policy might also have significant quantitative effect on measures of interest.

Let λ be the parameter of the exponentially distributed thinking time of both type 1 and 2 terminals (transitions t_1 and t_3) and μ the parameter of the exponentially distributed

state	*prs/prd*	*pri*	
		$\lambda < \mu$	$\lambda \geq \mu$
1	$\frac{\mu}{\mu + 2\lambda + 2\lambda^2}$	$\frac{\mu(\mu - \lambda)}{(\mu^2 + \lambda\mu + \lambda^2)}$	0
2	$\frac{\mu}{\mu + 2\lambda + 2\lambda^2} \cdot \frac{\lambda(2\lambda + \mu)}{\mu(\lambda + \mu)}$	$\frac{\lambda\mu(2\lambda + \mu)}{(\lambda + \mu)(\mu^2 + \lambda\mu + \lambda^2)}$	$\frac{\mu}{\lambda + \mu}$
3	$\frac{\mu}{\mu + 2\lambda + 2\lambda^2} \cdot \frac{\lambda}{\lambda + \mu}$	$\frac{\lambda\mu(\mu - \lambda)}{(\lambda + \mu)(\mu^2 + \lambda\mu + \lambda^2)}$	0
4	$\frac{\mu}{\mu + 2\lambda + 2\lambda^2} \cdot \frac{2\lambda^2}{\mu}$	$\frac{\lambda^2(\lambda + 2\mu)}{(\lambda + \mu)(\mu^2 + \lambda\mu + \lambda^2)}$	$\frac{\lambda}{\lambda + \mu}$

Table 1: Stationary behaviour with exponential firing time distribution

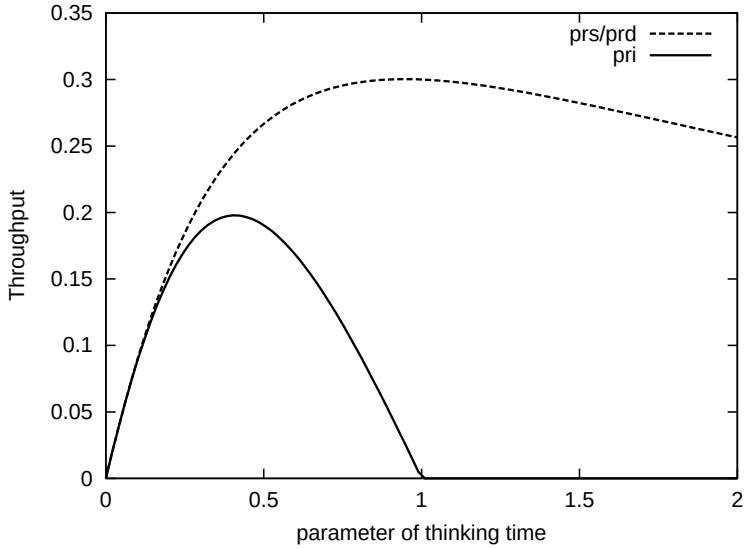

Figure 6: The steady state throughput of low priority customers ($\mu = 1$)

execution time of both type 1 and 2 jobs (transitions t_2 and t_4). The results of the analysis of stationary state probabilities [4] are summarized in Table 1.

The steady state throughput rate of low priority jobs (i.e., the average number of low priority jobs completed in a unit of time) is depicted in Figure 6 as a function of *lambda* when $\mu = 1$. This throughput measure can be obtained from the steady state distribution $(v_i, i = 1, 2, 3, 4)$ as $\rho_1 = \lambda(v_1 + v_3)$. The effect of the service policy becomes significant when the thinking time gets comparable with the execution time, i.e., $\lambda > 0.5\mu$. Figure 6 also indicates that the throughput of low priority jobs with prs/prd preemption policy reaches its maximum at around $\lambda = 1$ ($\max \rho_1 = 0.300283$ at $\lambda = 0.945027$) where the throughput with pri preemption policy vanishes.

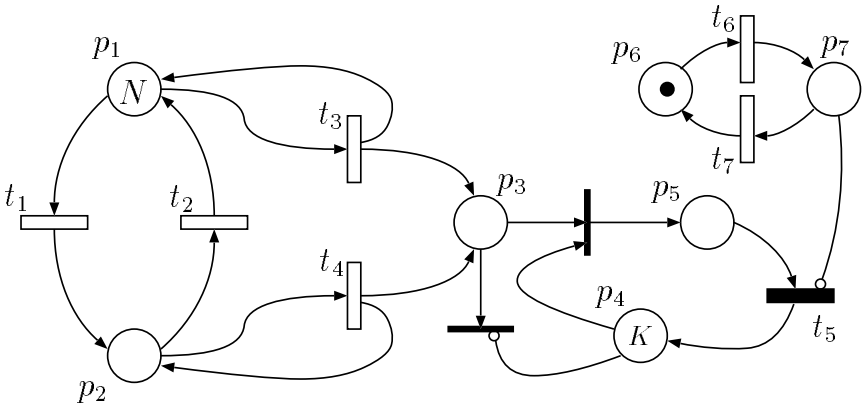

Figure 7: Transmission channel with failures

6.3 Noisy transmission channel

As a second example, we consider a noisy transmission channel that served as an example in [14] as well with different preemption policy. The NMPSN model of the channel is depicted in Figure 7. The data to be transmitted arrives to the channel from a Markovian source. The source is the superposition of N switched Poisson processes (SPP). Transitions t_1 and t_2 model the jumps between the states of the SPPs. Transitions t_3 and t_4 generates the data that will be transmitted on the channel. Transitions t_1, t_2, t_3 and t_4 have infinite-server semantics. The number of tokens in place p_5 represents the number of data packets in the system; no more than K packets may be present in the system simultaneously. The packets arriving when the system is full are lost. The transmission is represented by transition t_5; t_5 is single-server, pri type transition. The failure of the system is modeled by places p_6, p_7 and by transitions t_6, t_7; having a token in place p_7 the transmission (if any) is preempted.

The example was solved with the following numerical parameters:

- denoting the firing rate of EXP transition t_i by λ_i: $\lambda_1 = 0.02, \lambda_2 = 0.1, \lambda_3 = 0.4, \lambda_4 = 1.2, \lambda_6 = 0.1, \lambda_7 = 1$;
- the size of the system is defined by $N = 5$ and $K = 8$, as a result the model has 108 tangible markings;
- the time required to perform the transmission of a data packet is distributed uniformly in the interval $[0.5, 1.0]$;
- the step size of the discretization $d = 0.004$.

The size of the discretized state space is 2268060. To perform the transient analysis until 30 time units, the vector matrix multiplication has to be executed 30/0.004=7500 times which took about 3 hours.

Figure 8 and 9 show the transient probabilities of having x, $0 \leq x \leq K$ data packets in the system. Since the system is rather overloaded, the probability of having only a few packets in the system is close to 0 after the initial transient time.

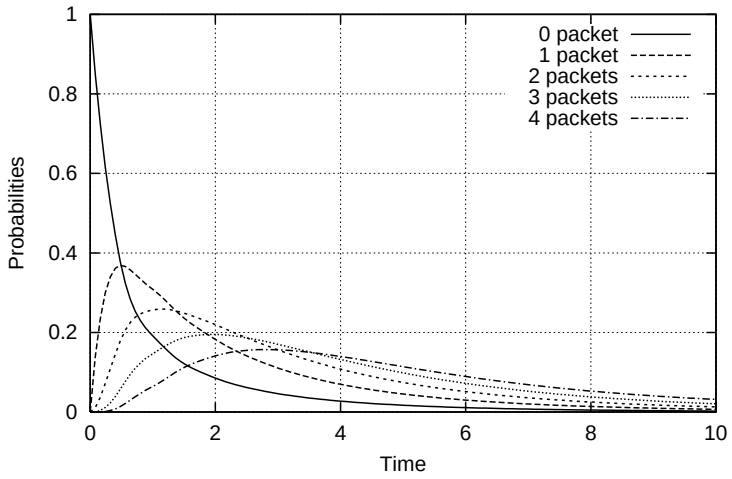

Figure 8: Probability of having x ($0 \leq x \leq 4$) data packets in the system

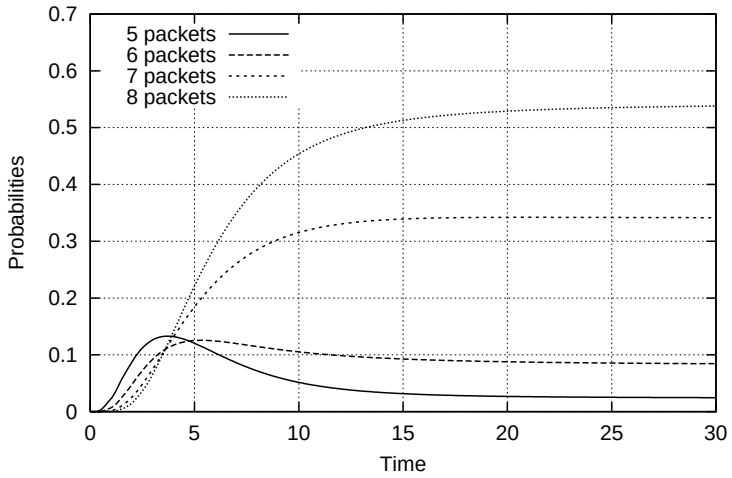

Figure 9: Probability of having x ($5 \leq x \leq K$) data packets in the system

The accuracy of the results obtained by the numerical procedure described in Section 5 were checked using a simulator and were found precise.

6.4 Queueing model with server maintenance periods

Figure 10 depicts the model of a queueing system. Arrivals occur according to Poisson-process represented by transition T_a. The queue has a buffer for K jobs, jobs arriving when the buffer is full are lost. End of the service of a job is represented by transition T_l. When the queue is empty maintenance of the service unit can start (transition T_s). End of maintenance is modeled by transition T_e which adopts pri memory policy. Possible preemption of the maintenance activity is represented by transitions T_{p1} and T_{p2}.

The example was solved by implementing an M/Ph/K/N queueing system with the following parameters:

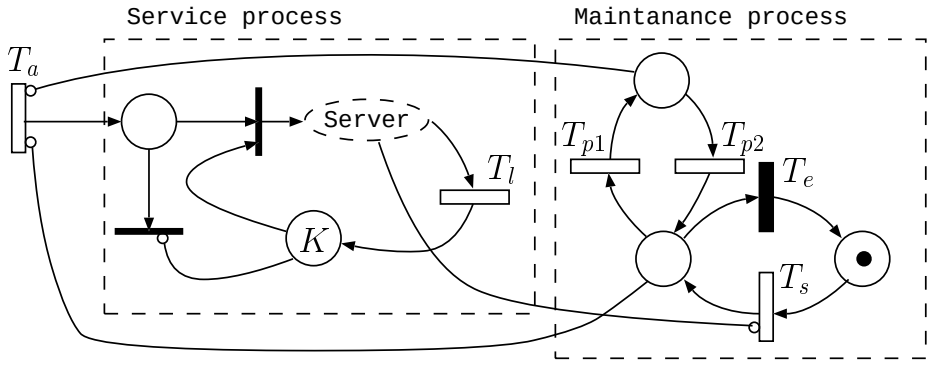

Figure 10: Queue with server maintenance periods

- arrival rate (transition T_a): 1.0,
- service time: 10-phase Erlang distribution with mean equals 4.5,
- number of servers $K = 5$, maximal number of jobs in the system $N = 25$,
- rate of transition T_s is 0.1, duration of maintenance period is uniformly distributed in the interval $[2, 3]$,
- preemption of the maintenance process starts with rate 0.2, maintenance restarts with rate 1.0.
- the step size of the discretization $d = 0.004$.

Figure 11 depicts the transient probabilities of the states when the system is empty. Figure 12 shows the transient probability of having x $(1 \leq x \leq 6)$ jobs in the system.

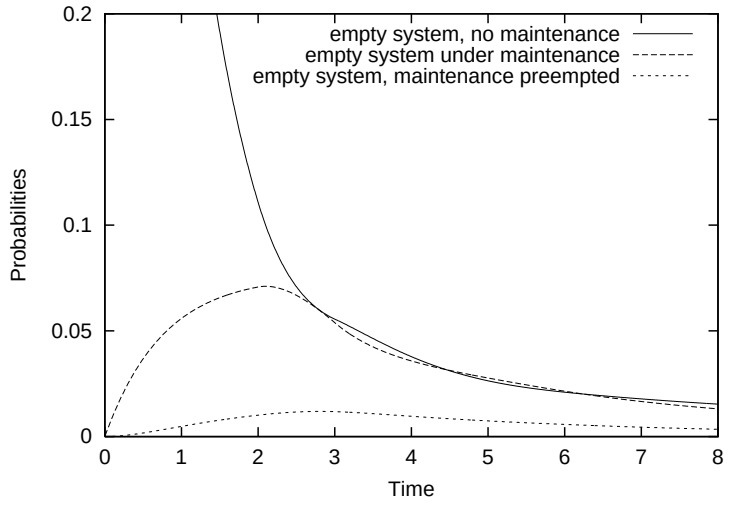

Figure 11: Probability of different states when the queue is empty

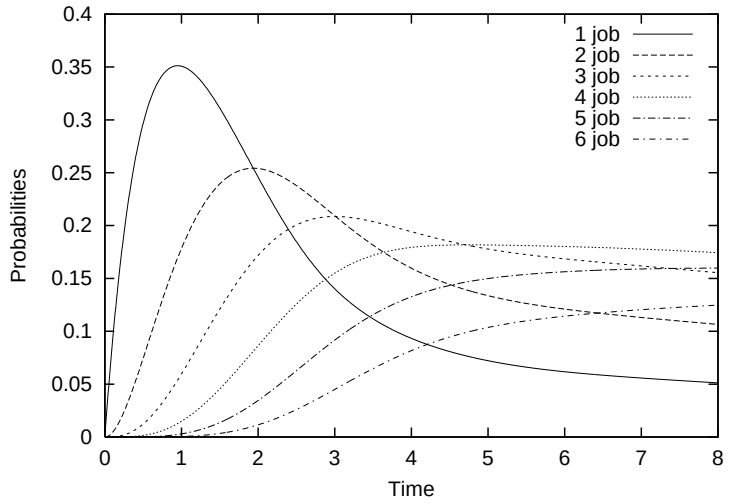

Figure 12: Probability of having x ($1 \leq x \leq 6$) jobs in the system

This model has about 2 million tangible markings. The size of the discretized state space is the number of tangible markings plus 157.000. The discretized state space is only slightly larger then the number of tangible markings because there are only two markings in which transition T_e is active. Since the discretized state space of this model is approximately as big as it is in the case of the model that was presented in Section 6.3, the amount of time needed to perform one step ahead in the transient analysis is approximately the same for the two models. In other words, the analysis of a model with 106 tangible markings might require the same amount of time (and memory) as the analysis of a model with 2 million markings. Indeed, an important conclusion can be drawn from the above examples. The applicability of the proposed technique cannot be decided based on the number of tangible markings of the model. It is the size of the underlying discretized state space that determines if the method can be applied or not.

7 Conclusion

The paper presented a set of partial and ordinary differential equations that describes the stochastic behavior of NMSPNs with pri type transitions with distinct sampled periods in "time domain". For the kernel representation of the stochastic process subordinated to the sampled period of a pri type transition the identity of the time domain and the previously known transform domain description was shown.

A numerical analysis method was proposed based on the obtained description. The applicability and the numerical properties of the proposed method were demonstrated through various examples.

The presented time domain analytical description of NMSPNs with pri transitions verifies the numerical method proposed in [15] as a first order approximation of time domain behavior.

References

[1] M. Ajmone Marsan, G. Balbo, A. Bobbio, G. Chiola, G. Conte, and A. Cumani. The effect of execution policies on the semantics and analysis of stochastic Petri nets. *IEEE Transactions on Software Engineering*, SE-15:832–846, 1989.

[2] M. Ajmone Marsan and G. Chiola. On Petri nets with deterministic and exponentially distributed firing times. In *Lecture Notes in Computer Science*, volume 266, pages 132–145. Springer Verlag, 1987.

[3] A. Bobbio, V.G. Kulkarni, A. Puliafito, M. Telek, and K. Trivedi. Preemptive repeat identical transitions in Markov Regenerative Stochastic Petri Nets. In *6-th International Conference on Petri Nets and Performance Models - PNPM95*, pages 113–122. IEEE Computer Society, 1995.

[4] A. Bobbio, A. Puliafito, and M. Telek. A modeling framework to implement combined preemption policies in MRSPNs. *IEEE Tr. on Software Engineering*, 26:36–54, Jan 2000.

[5] A. Bobbio and M. Telek. Combined preemption policies in MRSPN. In Ravi Mittal et al., editor, *Fault Tolerant Systems and Software*, pages 92–98. Narosa Pub. House, New Dehli - India, 1995.

[6] A. Bobbio and M. Telek. Markov regenerative SPN with non-overlapping activity cycles. In *International Computer Performance and Dependability Symposium - IPDS95*, pages 124–133. IEEE Computer Society Press, 1995.

[7] A. Bobbio and M. Telek. Non-exponential Stochastic Petri Nets: an overview of methodes and techniqueslicies. Tutorial, June 1997.

[8] Hoon Choi, V.G. Kulkarni, and K. Trivedi. Markov regenerative stochastic Petri nets. *Performance Evaluation*, 20:337–357, 1994.

[9] D.R. Cox. The analysis of non-markovian stochastic processes by the inclusion of supplementary variables. *Proceedings of the Cambridge Phylosophical Society*, 51:433–440, 1955.

[10] R. German. New results for the analysis of deterministic and stochastic Petri nets. In *International Computer Performance and Dependability Symposium - IPDS95*, pages 114–123. IEEE CS Press, 1995.

[11] R. German. *Performance analysis of communication systems: Modeling with non-Markovian stochastic Petri nets.* John Wiley and Sons, Chichester, 2000.

[12] R. German and C. Lindemann. Analysis of stochastic Petri nets by the method of supplementary variables. *Performance Evaluation*, 20:317–335, 1994.

[13] R. German and M. Telek. Towards a foundation of the analysis of Markov Regenerative Stochastic Petri Nets. In *PNPM '99*, pages 64–73, Zaragoza, Spain, Sept 1999. IEEE CS Press.

[14] A. Heindl and R. German. A fourth-order algorithm with automatic stepsize control for the transient analysis of DSPNs. In *7-th International Conference on Petri Nets and Performance Models - PNPM97*, pages 60–69. IEEE Computer Society, 1997.

[15] A. Horváth, A. Puliafito, M. Scarpa, and M. Telek. A discrete time approach to the analysis of non-Markovian stochastic Petri nets. In *Tools 2000*, pages 171–187, Schaumburg, IL, USA, March 2000. Springer, LNCS 1786.

[16] R. Marie and K.S. Trivedi. A note on the effect of preemptive policies on the stability of a priority queue. *Information Processing Letters*, 24:397–401, 1987.

[17] M. Telek, A. Bobbio, L. Jereb, A. Puliafito, and K. Trivedi. Steady state analysis of Markov regenerative SPN with age memory policy. In H. Beilner and F. Bause, editors, *8-th International Conference on Modeling Techniques and Tools for Computer Performance Evaluation, Lecture Notes in Computer Science*, volume 977, pages 165–179. Springer Verlag, 1995.

[18] M. Telek and A. Horváth. Transient analysis of age-MRSPNs by the method supplementary variables. *Performance Evaluation*, 45(4):205–221, 2001.

Appendix A

Partitioning of matrix $\boldsymbol{Q}$:

$$\boldsymbol{Q} = \left[\begin{array}{c|c|c||c|c|c} \boldsymbol{Q}^{M} & \boldsymbol{Q}^{M\mathcal{E}_1} & \boldsymbol{Q}^{M\mathcal{D}_1} & \cdots & \boldsymbol{Q}^{M\mathcal{E}_n} & \boldsymbol{Q}^{M\mathcal{E}_n} \\ \hline\hline & \boldsymbol{Q}^{\mathcal{E}_1} & \boldsymbol{Q}^{\mathcal{E}_1\mathcal{D}_1} & \cdots & & \\ \hline & \boldsymbol{Q}^{\mathcal{D}_1\mathcal{E}_1} & \boldsymbol{Q}^{\mathcal{D}_1} & \cdots & & \\ \hline\hline & & & \ddots & & \\ \hline\hline & & & \cdots & \boldsymbol{Q}^{\mathcal{E}_n} & \boldsymbol{Q}^{\mathcal{E}_n\mathcal{D}_n} \\ \hline & & & \cdots & \boldsymbol{Q}^{\mathcal{D}_n\mathcal{E}_n} & \boldsymbol{Q}^{\mathcal{D}_n} \end{array}\right]$$

The filter matrices $\boldsymbol{R}^{M}, \boldsymbol{R}^{E}, \boldsymbol{R}^{D}$ are defined as

$$\boldsymbol{R}^{M} = \left[\begin{array}{c|c|c||c|c|c} \boldsymbol{I}^{M} & & & \cdots & & \\ \hline\hline & \mathbf{0}^{\mathcal{E}_1} & & \cdots & & \\ \hline & & \mathbf{0}^{\mathcal{D}_1} & \cdots & & \\ \hline\hline & & & \ddots & & \\ \hline\hline & & & \cdots & \mathbf{0}^{\mathcal{E}_n} & \\ \hline & & & \cdots & & \mathbf{0}^{\mathcal{D}_n} \end{array}\right]$$

$$\boldsymbol{R}^E = \begin{bmatrix} \mathbf{0}^M & & & \cdots & & \\ & \boldsymbol{I}^{\mathcal{E}_1} & & \cdots & & \\ & & \mathbf{0}^{\mathcal{D}_1} & \cdots & & \\ & & & \ddots & & \\ & & & \cdots & \boldsymbol{I}^{\mathcal{E}_n} & \\ & & & \cdots & & \mathbf{0}^{\mathcal{D}_n} \end{bmatrix}$$

$$\boldsymbol{R}^D = \begin{bmatrix} \mathbf{0}^M & & & \cdots & & \\ & \mathbf{0}^{\mathcal{E}_1} & & \cdots & & \\ & & \boldsymbol{I}^{\mathcal{D}_1} & \cdots & & \\ & & & \ddots & & \\ & & & \cdots & \mathbf{0}^{\mathcal{E}_n} & \\ & & & \cdots & & \boldsymbol{I}^{\mathcal{D}_n} \end{bmatrix}$$

Using this filter matrices we defined the following matrices of size $|\mathcal{S}| \times |\mathcal{S}|$:

$$\begin{array}{l} \boldsymbol{Q}^M = \boldsymbol{R}^M \boldsymbol{Q} \boldsymbol{R}^M,\ \boldsymbol{Q}^{ME} = \boldsymbol{R}^M \boldsymbol{Q} \boldsymbol{R}^E,\ \boldsymbol{Q}^{MD} = \boldsymbol{R}^M \boldsymbol{Q} \boldsymbol{R}^D, \\ \boldsymbol{Q}^E = \boldsymbol{R}^E \boldsymbol{Q} \boldsymbol{R}^E,\ \boldsymbol{Q}^{ED} = \boldsymbol{R}^E \boldsymbol{Q} \boldsymbol{R}^D, \\ \boldsymbol{Q}^D = \boldsymbol{R}^D \boldsymbol{Q} \boldsymbol{R}^D,\ \boldsymbol{Q}^{DE} = \boldsymbol{R}^D \boldsymbol{Q} \boldsymbol{R}^E \end{array}$$

The $\boldsymbol{\Delta}$ matrix is decomposed similarly:

$$\boldsymbol{\Delta}^M = \boldsymbol{R}^E \boldsymbol{\Delta} \boldsymbol{R}^M,\ \boldsymbol{\Delta}^E = \boldsymbol{R}^E \boldsymbol{\Delta} \boldsymbol{R}^E,\ \boldsymbol{\Delta}^D = \boldsymbol{R}^E \boldsymbol{\Delta} \boldsymbol{R}^D,$$

Matrix $\boldsymbol{f}(y)$ is composed by the firing time distribution of the pri type transitions:

$$\boldsymbol{f}(y) = \begin{bmatrix} \mathbf{0}^M & & & \cdots & & \\ & f_1(y)\boldsymbol{I}^{\mathcal{E}_1} & & \cdots & & \\ & & f_1(y)\boldsymbol{I}^{\mathcal{D}_1} & \cdots & & \\ & & & \ddots & & \\ & & & \cdots & f_n(y)\boldsymbol{I}^{\mathcal{E}_n} & \\ & & & \cdots & & f_n(y)\boldsymbol{I}^{\mathcal{D}_n} \end{bmatrix}$$